Molecular Biology: Open Access
ISSN: 2168-9547

Rytty et al., Mol Biol 2014, 3:1
DOI: 10.4172/2168-9547.1000117

Research Article Open Access

Functional MRI in Patients with the *C9ORF72* Expansion Associate Frontotemporal Dementia

Rytty Riikka[1,2], Nikkinen Juha[3], Suhonen Noora[1,2], Moilanen Virpi[2], Renton Alan E[4], Traynor Bryan J[4], Tervonen Osmo[3], Kiviniemi Vesa[3]* and Remes Anne M[5]*

[1]*Institute of Clinical Medicine, Neurology, University of Oulu, Oulu, Finland*
[2]*Department of Neurology, Oulu University Hospital, Oulu, Finland*
[3]*Institute of Clinical Medicine, Radiology, University of Oulu, Oulu, Finland*
[4]*Neuromuscular Diseases Research Unit, Laboratory of Neurogenetics, National Institute on Aging, National Institutes of Health, USA*
[5]*Institute of Clinical Medicine, Department of Neurology, University of Eastern Finland, and Kuopio University Hospital, Kuopio, Finland*

Abstract

Functional MRI studies have revealed connectivity changes in several brain networks in patients with neurodegenerative diseases and imaging genomics is an emerging field to investigate the role of genetics in brain function. A hexanucleotide repeat expansion in open reading frame in chromosome 9 (*C9ORF72*) is a common cause of familial frontotemporal dementia. The aim of this study was to evaluate resting state networks in behavioral variant frontotemporal dementia (bvFTD) patients with the *C9ORF72* expansion by using functional MRI. Seven patients and matched healthy controls were examined. The group specific resting state networks were identified by independent component analysis and the dual regression technique was used to detect between-group differences in the resting state networks with $p<0.05$ threshold corrected for multiple comparisons. Increased anti-correlation between bilateral thalamic parts of the salience network and anterior sub-network of the Default mode network (DMN) was found in patients with the *C9ORF72* expansion. In addition, increased resting state connectivity was detected in the right-sided dorsal attention network. The changes in these cognitive networks may explain executive dysfunction as well as neuropsychiatric symptoms in patients with bvFTD.

Keywords: Resting State; Fmri Apathy; Imaging Genetics; Frontotemporal Lobar Degeneration; Dementia; Thalamus

Introduction

Frontotemporal lobar degeneration (FTLD) is a clinically and genetically heterogeneous group of neurodegenerative disorders characterized by behavioral and language deficits. The most common clinical presentation is behavioral variant frontotemporal dementia (bvFTD), which is characterized by profound changes in behavior and personality and decline in executive functions [1,2]. A positive family history is present in up to 40-50% of FTLD cases [1]. Mutations in progranulin (*PGRN*), the microtubule associated protein tau (*MAPT*) genes and a hexanucleotide repeat expansion in open reading frame in chromosome 9p21 (*C9ORF72)* have been found to explain a majority of familial FTLD [3-5].

Integrity of the brain's functional network dynamics is crucial for normal functioning [6]. Resting state functional MRI (rfMRI) can be used to study the intrinsic connectivity of functional brain networks in task-free settings by mapping temporally synchronous, spatially distributed, spontaneous low frequency (<0.08 Hz) blood-oxygen level-dependent (BOLD) signal fluctuations [7,8]. It provides an indirect marker of neuronal function on a timescale of seconds with high spatial resolution [6].

The salience network is a large-scale network that bridges the frontal lobes and limbic system and is related to socially-emotionally relevant information processing [9]. It consists of the anterior cingulate cortex (ACC), orbital frontoinsula (FI), striatum, thalamus and amygdala - areas affected by FTLD related neuropathology [9,10]. The anti-correlated DMN is instead a posterior network that consists of the hippocampi, posterior cingulate cortex / precuneus, lateral parietal regions and the rostromedial prefrontal cortex and has been associated with task-independent thought processes and episodic memory function [11]. Alzheimer's disease (AD) related atrophy and hypometabolism is mainly located in the areas associated with the DMN [10]. Since these two networks account for the most essential cognitive symptoms and also the sites of neuropathology of bvFTD and AD, they have received most interest in the fMRI studies of neurodegenerative dementias. Reduced DMN connectivity in patients with AD has been a quite consistent finding across studies [12,13]. There are only few studies available of bvFTD and the results have been less consistent. However, decreased functional connectivity in the salience network has been the most frequent finding in bvFTD. In some studies increased connectivity in the DMN has been observed, but there has been a lot of variation concerning the DMN related findings in bvFTD [12, 14, 15-18].

Clinical diagnosis of bvFTD is often challenging because there is considerable heterogeneity in symptology, but genetic testing has provided great advances in the diagnostics. Imaging genomics is an emerging field investigating the role of genes in brain function [19]. There are only a few reports available of resting state brain networks using rfMRI in genetically determined FTLD patients or asymptomatic mutation carriers [15,16,20]. These studies have shown that functional changes are present in the brain already before atrophy can be detected on structural MRI and even before symptom onset [15,16,20]. In a small study of clinically affected bvFTD patients with *PGRN*-mutation a decrease in the salience network connectivity and an increase in the DMN connectivity was detected [15].

Our aim was to analyze the whole brain cortex resting state networks in bvFTD patients with the *C9ORF72* expansion. Given the location of the salience network in the areas of bvFTD related

***Corresponding author:** A.M. Remes, Department of Neurology, Institute of Clinical Medicine, University of Eastern Finland, P.O.Box 1627, 70211 Kuopio, Finland, Tel : +358 44 717 4655 ; Fax : +358 17 172305; E-mail: anne.remes@uef.fi

Received June 24, 2014; **Accepted** July 21, 2014; **Published** July 25, 2014

Citation: Rytty R, Nikkinen J, Suhonen N, Moilanen V, Renton AE, et al. (2014) Functional MRI in Patients with the *C9ORF72* Expansion Associate Frontotemporal Dementia. Mol Biol 3: 117. doi:10.4172/2168-9547.1000117

neurodegeneration and its involvement in behavioral and emotional functions, we hypothesized to find functional connectivity decrease in this network in this genetically uniform bvFTD patient group.

Methods

Subjects

In this study seven bvFTD patients with the *C9ORF72* expansion (4 male, 3 female) and eight gender and age-matched controls were examined (Table 1).Mutations in *PGRN* and *MAPT* were excluded. The *C9ORF72* expansion was analysed using the repeat-primed PCR assay [5]. Patients were examined in Oulu University Hospital, the Memory Clinic of the Department of Neurology.

Diagnosis of bvFTD was done according Neary criteria and all of the patients also fulfilled Rascovsky criteria for bvFTD [1,2]. Patients with logopenic aphasia and semantic dementia were excluded from the cohort. Mean age of the patients was 58 years (47-67 years) (Table 1). MMSE score was 26-30 (mean 27.6). Neuropsychological evaluation and modified frontal behavioural inventory (FBI-mod) were performed on all patients. The most prevalent neuropsychiatric symptoms in FBI-mod were irritability, loss of insight, disorganization and apathy. In neuropsychological evaluation executive dysfunction was present in all patients. Three patients (43 %) had mild to moderate executive dysfunction and four patients (57 %) had severe executive impairment. Impairment in episodic memory was detected in three patients (43 %). Profound deficits in delayed recall were not detected in any of the patients. Severity of bvFTD was rated mild in three patients, moderate in three patients and severe in one patient [21]. None of the patients had symptoms or signs suggesting amyotrophic lateral sclerosis. All control subjects (n=8, mean age 56.9 years, 5 male) were interviewed and examined. Psychiatric and neurological disorders and medications affecting the central nervous system were excluded. Beck´s depression inventory (BDI) (mean 1.9/63) and MMSE (mean 29.3) were performed on the control group to rule out depression and memory deficits. Written informed consent was obtained from all the patients or their guardians and control cases. The research protocols were approved by the Ethics Committees of the Northern Ostrobothnia Hospital District.

Imaging methods

Resting-state BOLD data were collected on a GE 1.5 T Hdxt with GE's standard eight channel receiver head coil. Subjects were imaged with conventional gradient recalled echo (GRE) EPI sequence TR 1800 ms, TE 40 ms, 253 time points, 28 oblique axial slices, slice thickness 4 mm, inter-slice space 0.4, covering the whole brain, field of view (FOV) 25.6 cm x 25.6 cm, with 64 x 64 matrix yielding 4x4x4 mm voxels with 0.4 mm gap in between, and a flip angle of 90º. The first three images were excluded from the time series due to T1 relaxation effects. T1-weighted scans were imaged using 3D fast spoiled gradient echo (FSPGR) BRAVO sequence (TR 12.1ms, TE 5.2 ms, slice thickness 1.0 mm, FOV 24.0 cm, matrix 256 x 256 (i.e. 1 mm cubic voxels), and flip angle 20º, parallel imaging factor 2 and number of excitations (NEX) 0.5 in order to obtain anatomical images for co-registration of the fMRI data to standard space coordinates. The subjects were asked to relax and lie still without thinking anything special, and look at a cross through the scanner mirror on a screen provided by custom-made video projector apparatus. Motion was minimized using soft pads fitted over the ears and hearing was protected with ear plugs and pads.

Pre-processing of imaging data

Data pre-processing was carried out in the framework of Oxford Centre for Functional MRI of the Brain (FMRIB) Software Library (FSL) 4.1 software (www.fmrib.ox.ac.uk/fsl/). Head motion in the fMRI data was corrected using multi-resolution rigid body co-registration of volumes, as implemented in motion correction with fast linear registration tool (MCFLIRT) [22]. The default settings used were: middle volume as reference, a three-stage search (8 mm rough + 4 mm, initialized with 8 mm results + 4 mm fine grain, initialized with the previous 4 mm step results) with final tri-linear interpolation of voxel values, and normalized spatial correlation as the optimization cost function. Brain extraction was carried out for motion corrected BOLD volumes with optimization of the deforming smooth surface model, as implemented in Brain Extraction Tool (BET) software [23] using threshold parameters f = 0.5 and g = 0; and for 3D FSPGR volumes, using parameters f = 0.25 and g = 0. This procedure was verified with visual inspection of the extraction result. When the BET failed to satisfactorily remove some tissue, the extra cranial tissues (often in neck areas) were removed manually by removing the tissue with FSL and then re-entering the data into the processing pipeline.

After successful brain extraction the BOLD volumes were spatially smoothed; 5 mm Full Width with Half Maximum (FWHM) Gaussian kernel and voxel time series were detrended using a Gaussian linear high-pass filter with a 100 second cutoff. Fslmaths tool was used for these steps. Multi-resolution affine co-registration as implemented in the Fast Linear Registration Tool (FLIRT) [22] was used to co-register mean non-smoothed fMRI volumes to 3D FSPGR volumes of corresponding subjects, and 3D FSPGR volumes to the Montreal

						Neuropsychological profile											
Case	Gender	Age at onset	Age at fMRI	MMSE	FBI	VIQ	PIQ	Digit span fwd	Digit span bwd	Immediate recall	Delayed recall	Visual memory	Semantic Fluency	Phonemic Fluency	TMT A	TMT B	REY figure copy
1	f	45	50	28	19	94	87	6	4	13	9	18	ND	14	ND	120	34
2	f	50	52	28	32	90	83	7	3	14	10	18	20	ND	73	139	18
3	m	55	63	30	22	90	75	6	3	14	14	19	18	ND	66	170	20
4	f	59	61	26	20	84	58	6	4	9	8	ND	12	3	150	IC	28
5	m	45	47	27	25	79	94	5	4	12	9	15	13	8	48	163	32
6	m	65	67	26	27	65	59	4	3	6	4	ND	9	1	99	IC	26
7	m	51	66	28	5	90	99	5	4	4	4	14	23	ND	70	IC	34
Mean (sd)		52.9	58.0	27.6	21.4	100 (15)	100 (15)	5.9 (1.0)	4.1 (0.8)	14.8 (3.3)	13.6 (3.4)	20.8 (3.1)	23.5 (5.8)	15.8 (6.4)	41.4 (17.2)	82.3 (26.7)	32.2 (3.7)

All test data except IQ scores is represented as raw scores. Mean and standard deviation for middle-aged healthy controls are shown. MMSE = Mini-Mental State Examination; FBI = Frontal Behavioral Inventory; VIQ = Wechsler Adult Intelligence Scale Verbal IQ; PIQ = Wechsler Adult Intelligence Scale Performance IQ; Immediate and delayed recall = Wechsler Memory Scale, Logical Memory; Visual memory = Benton Visual Retention Test, Version C; TMT A & B = Trail Making Test, Part A & B; REY = Rey-Osterrieth Complex Figure Test; ND = Not done; IC = Not able to complete the test

Table 1: Subject demographics.

Neurological Institute (MNI) standard structural space template (MNI152_T1_2mm_brain template included in FSL). Tri-linear interpolation was used, a correlation ratio was used as the optimization cost function, and regarding the rotation parameters a search was done in the full [-π π] range. The resulting transformations and the tri-linear interpolation were used to spatially standardize smoothed and filtered BOLD volumes to the 4 mm MNI standard space. Anatomical data was dimension swapped and manually checked for brain extractions and further analysed for voxel based morphometry (VBM) with FSL steps fslvbm 2-3 for group differences. Also a voxel-wise gray matter regressor was produced with FSL 4.1 from 1 mm into 4 mm cubic voxel gray matter regressor matching the 4 mm cubic BOLD data in order to minimize the effects of gray matter loss.

ICA analysis

Spatial ICA analysis was carried out using FSL 4.1 MELODIC implementing probabilistic independent component analysis (PICA) [24]. Multisession temporal concatenation tool in MELODIC was used to perform PICA related pre-processing and data conditioning in group analysis setting. Spatial ICA using a conventional 30 independent components (ICs) was applied to detect resting state networks as described earlier [25-27]. The between-subject analysis of the resting data was carried out using a regression technique (dual regression) that allows for voxel-wise comparisons of RSNs [26,28].

Dual regression approach identifies subject-specific temporal dynamics and associated spatial maps within each subject's fMRI data set. This involves (A) using the group-ICA spatial maps in a linear model fit against the separate fMRI data sets, resulting in matrices (time-course matrices) describing temporal dynamics for each component and subject, and (B) using these time-course matrices to estimate subject-specific spatial maps. Finally, the different component maps are collected across subjects into single 4D files (1 per original ICA map) and tested voxel-wise for statistically significant differences between groups using non-parametric permutation testing with randomize in FSL, with exhaustive 6435 permutations (n=15) [29]. The dual regression was performed in two ways; with and without variance normalization in order to see whether the differences between the groups were more related to spatial (no variance normalization) or amplitude of the signal (variance normalized) [30]. Experienced researcher (VK) identified 19 RSNs. The data was thresholded using a $p<0.05$, corrected for family-wise errors for each RSN map separately at voxel level. Individual gray matter segmentation map was used at the voxel level in order to regress out the gray matter lose effects with --vx f -option in dual regression randomize run. We also adjusted for the more stringent risk of type 1 error (false positives) induced by selecting multiple RSNs. In short it means that the ttemporally concatenated subject-specific maps of each IC created by the initial dual-regression run were spatially concatenated in the y-direction and then randomise run 6435 fully exhaustive random permutations on the concatenated map (15 subjects's data temporally concatenated with 19 ICs spatially concatenated y-direction [31]. The resulting statistical between-group difference map was thresholded at $p<0.05$ (corrected for family-wise errors within and between all concatenated RSN maps), re-sampled into 2 mm, and then divided into 19 ICs.

The resulting ICA maps were sub-sampled into 2 mm MNI-space. The Juelich histological atlas, and the Harvard –Oxford cortical and subcortical atlases (Harvard Center for Morphometric Analysis) provided with the FSL4 software were used to quantify the anatomical characteristics of the resulting difference maps. Mean absolute and relative motion estimates showed no differences between the groups, paired t-test $p = 0.9$ and $p = 0.35$, respectively.

Results

Default mode network: Increased anti-correlation (i.e. inverse correlation) between bilateral thalamic regions (parts of the salience network) and the DMN anterior sub-network was detected in variance normalized dual regression analysis in patients with the *C9ORF72* expansion when compared to healthy controls (Table 2, Figure 1A). When analyzing without variance normalization, there was also abnormal anatomical spread of the anti-correlation in patients with the *C9ORF72* expansion compared to controls (Figure 1B). The anatomically weighted (a.k.a dual regression results without variance normalization) changes in the network neighbored and partially overlapped the connectivity related changes (Figure 1C). These changes in the thalamic regions were focused on right hemisphere in areas with predominant pre-frontal white matter connectivity, based on the FSL thalamic projection probability map. Another cluster of changes in both resting state connectivity and anatomical spread of RSN was noticed in left precuneus in superior parietal lobule (Table 2). Decrease of anatomical spread without change in functional connectivity was detected in left temporo-occipital fusiform gyrus and in parahippocampal gyrus.

Dorsal Attention Network (DAN): Increased functional resting state connectivity was detected in the right-sided DAN in right inferior frontal gyrus in patients with the *C9ORF72* expansion compared to controls (Figure 1A). Analysis without variance normalization showed abnormal anatomical spread of the DAN in left nucleus accumbens and right ACC in the *C9ORF72* expansion carriers (Figure 1B). The anatomical and connectivity related changes were in distinct anatomical structures (Figure 1A, 1B, Table 2).

Other networks: There were no changes in the salience network without variance normalization. However, with variance normalized analysis mild increase in spontaneous brain connectivity in left visual cortex V4 was detected (Figure 1A). A RSN focused on middle temporal gyrus bilaterally showed abnormal anatomical spread but no connectivity related changes of the RSN in patients with the *C9ORF72* expansion, in left superior frontal gyrus in pre-motor areas (Figure 1B, Table 2). Y-concatenation correction for multiple ICA components was also performed, but no statistically significant changes were detected using this more stringent correction.

			MNI-coordinate of Max t-score		
IC	# voxels	Max t-score	X	Y	Z
Change in resting state connectivity (variance normalization)					
Salience	1	6.6	30	11	16
DMN ant	11	7.1	21	29	19
DAN R	1	6.5	9	37	17
Change in anatomical spread of connectivity (no variance normalization)					
DMN ant	8	6.7	27	18	31
Middle temporal gyrus	3	7.6	28	34	33
DAN R	2	11.2	25	34	15

Table 2: Functional brain regions showing altered functional connectivity in patients with the *C9ORF72* expansion compared to healthy controls. In variance normalized dual regression analysis the DMN showed abnormal anti-correlation (i.e. inverse correlation) between bilateral thalamic regions and the DMN anterior sub-network. Salience network and right-sided DAN showed increased resting state activity. Without variance normalization three IC's (DMN ant, middle temporal gyrus, DAN R) showed abnormal anatomical spread of the RSN.

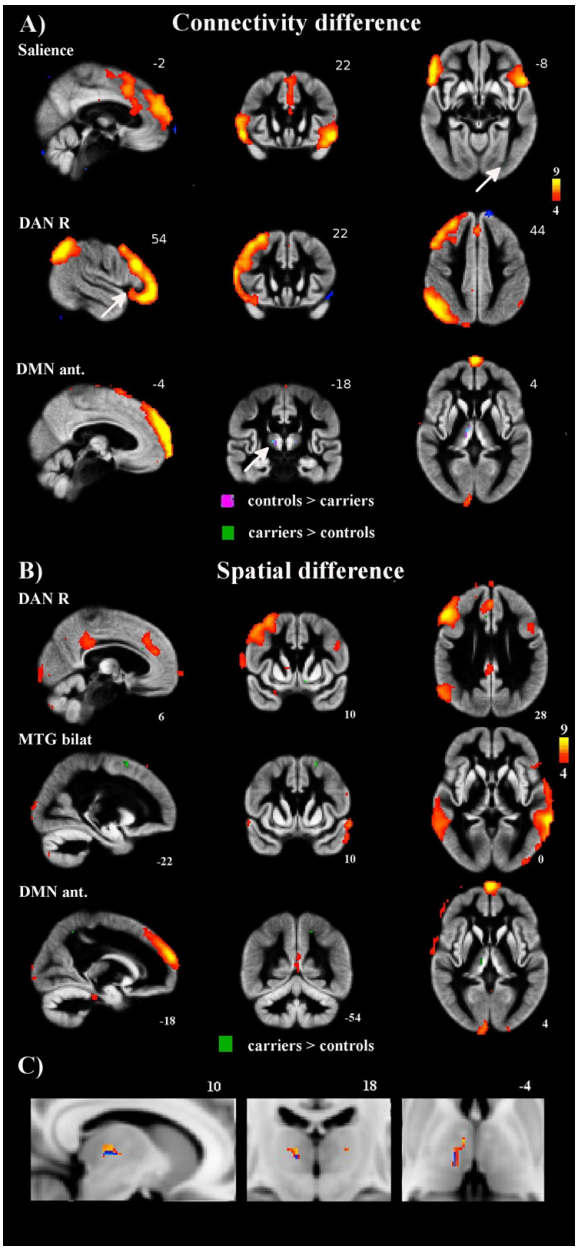

Figure 1: A) Resting state networks showing altered resting state connectivity in patients with the *C9ORF72* expansion associated bvFTD in variance normalized dual regression analysis. ICA maps of the resting state networks are shown in red-yellow colors with z-score thresholding shown by color bar in right. Increased anti-correlation between the DMN anterior sub-network and bilateral dorso-medial thalamic nuclei (parts of the salience network) is shown in purple. Increased functional connectivity in the patient group is shown in green color. The differences between groups are corrected for multiple comparisons, threshold $p < 0.05$ for voxel level and gray matter VBM maps were used as regressors to reduce the effects of gray matter loss.
B) Resting state networks showing abnormal anatomical spread of connectivity in patients with the *C9ORF72* expansion associated bvFTD. The color encoding and analysis is otherwise the same as in Figure 1A except for the lack of variance normalization in dual regression analysis, which makes the analysis more sensitive to anatomical rather than BOLD amplitude differences. MTG bilat= bilateral middle temporal gyrus.
C) A close-up combining the results with (yellow) and without (blue) variance normalization. The DMN showed increased anti-correlation between bilateral thalamic regions of the salience network and the DMN anterior sub-network (yellow) neighboring with abnormal anatomical spread of the DMN connectivity with the thalamic areas (blue) in patients with the *C9ORF72* associated bvFTD.

Voxel based morphometry of gray matter: VBM randomize analysis ($p<0.05$ corrected for multiple comparisons) showed atrophy of gray matter pre-dominantly in right frontal lobe and left temporo-parietal regions in patients with the *C9ORF72* expansion (Figure 2, Table 3). In the frontal areas the atrophy was the most dominant in frontobasal regions and frontal pole. Atrophy was also detected in right parahippocampal areas. In the left dominant hemisphere atrophy was detected in auditory areas, pre-motor, and sensorimotor cortices. Mild gray matter atrophy was found also in the left supramarginal gyrus and posterior cingulate gyrus.

Discussion

This is the first report of rfMRI in patients with the *C9ORF72* associated bvFTD. We found increased anti-correlation between the DMN and the salience network in bvFTD patients with the *C9ORF72* expansion. Abnormal anatomical spread of the anti-correlation in bilateral thalamic areas with the DMN anterior sub-network was also detected. The anatomical and signal amplitude changes were detected in neighboring anatomical structures. Until now, only one rfMRI study of genetically determined and clinically affected FTLD patients with mutations in the *PGRN* has been published and decreased salience network connectivity and increased DMN connectivity was found [15]. The other studies of genetically determined bvFTD have been conducted on presymptomatic patients and the results are contradictory (Table 4) [16,20].

The DMN and the salience network are considered to be anti-correlated in a healthy brain [32,33]. In the present study the patients with the *C9ORF72* expansion had increased anti-correlation between bilateral dorso-medial thalamic nuclei and the DMN. The dorso-medial thalamic nuclei have been suggested to represent a key node binding the salience network circuitry together [9]. These nuclei play a role in numerous behavioral functions including motivation and drive, memory, emotional experience and expression, executive functions and attention [34]. A gray matter atrophy of the medial thalamus has been previously detected in patients with the *C9ORF72* expansion [35,36]. We used gray matter volumes as regressors to minimize the effects of atrophy on the functional connectivity analysis and hence the present finding of increased anti-correlation is not due to atrophy. Decreased connectivity in the anterior thalamus and elevated prefrontal cortex connectivity have been shown to associate with greater levels of apathy in FTLD patients [18]. Apathy was also a prominent neuropsychiatric symptom in our patients. Thus functional and structural changes in

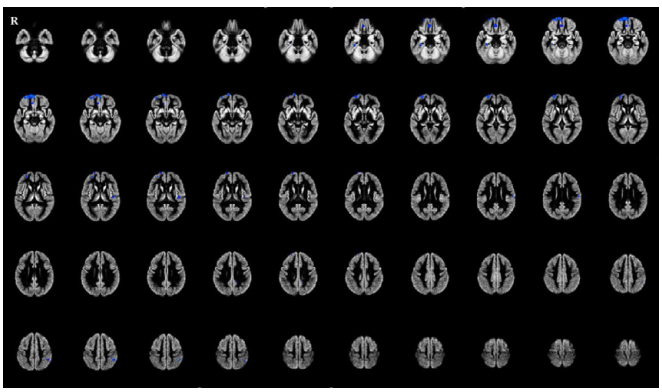

Figure 2: Regional atrophy was detected mainly in right frontal and left temporal areas in the patient group (blue) compared with 16 healthy age-matched controls, threshold $p < 0.05$.

# Voxels	Mean T-score	Sem T-score	Max T-score	Max X	Max Y	Max Z	Side and anatomical area
647	3.54	0.01	4.72	2	58	-12	R Frontal pole
137	3.50	0.02	4.11	4	36	-20	R Frontal medial cortex, BA 25
49	4.56	0.06	5.41	32	-28	-22	R Temporal parahippocampus
43	4.15	0.03	4.70	-42	-20	12	L Heschl's gyrus, secondary somatosensory cortex
34	3.53	0.05	4.14	18	66	14	R Frontal pole
34	4.53	0.06	5.52	-48	-44	50	L Supramarginal gyrus
11	5.03	0.09	5.54	-56	-18	24	L Precentral gyrus; primary motor cortex
9	4.18	0.04	4.35	22	50	36	R Frontal pole
7	5.32	0.06	5.63	-12	-42	34	L Posterior cingulate gyrus
7	4.42	0.06	4.75	-38.0	-36	50	L Postcentral gyrus; somatosensory cortex

P-values from corrp-tstat1.
R right, L left

Table 3: Regional atrophy detected in structural MRI.

Study group	DMN ant.	DMN post.	Salience	Executive	DAN	ATT/WM	Reference
Asymptomatic MAPT *(n=8)*	-	+	0	NS	NS	NS	Whitwell et al 2011
Asymptomatic PGRN *(n=28)* and MAPT *(n=9)*	0	0	-	NS	NS	NS	Dopper et al 2013
Asymptomatic PGRN *(n=9)*	0	0	+	NS	NS	NS	Borroni et al 2011
FTLD PGRN *(n=7)*	0	+	-	NS	NS	NS	Borroni et al 2011
bvFTD *(n=19)*	+	+	0	0	+	0	Rytty et al 2013
bvFTD *(n=21)*	-	+	-	NS	NS	NS	Whitwell et al 2011
bvFTD *(n=12)*	0	+	-	NS	NS	NS	Zhou et al 2010
bvFTD *(n=12)*	0	0	-	0	0	+/-	Filippi et al 2012
bvFTD *(n=8)*	+	+	+/-	+	NS	NS	Farb et al 2012

MAPT: microtubule associated protein tau mutation carriers
PGRN: progranulin mutation carriers
0: No changes in functional connectivity
+: Increased functional connectivity
-: Decreased functional connectivity
NS: Not studied
DMN ant: Anterior parts of the Default mode network
DMN post: Posterior parts of the Default mode network
DAN: Dorsal attention network
ATT/WM: Attention/working memory network

Table 4: The rfMRI-findings in previous studies of patients with FTLD.

thalamus may explain executive dysfunction and also neuropsychiatric profile of patients.

There are only few reports available about other brain networks than the DMN and the salience network in patients with neurodegenerative diseases. When analyzing the whole brain cortex resting state networks, we found increased connectivity in the right-sided DAN in patients with the *C9ORF72* expansion. The DAN appears to be responsible for voluntary (top-down) attention orienting as well as the preparation and selection for stimuli and responses [37,38]. We have previously reported increased connectivity in the left DAN in a patient group that consisted of both sporadic and genetically confirmed bvFTD [17]. However, Filippi with colleagues did not find any changes in the DAN and there are no other reports available [14].

In the present study increased connectivity was also detected in the salience network; which is controversial to the hypothesis of decreased connectivity in the salience network in patients with bvFTD. However, previous findings associated with the salience network have been somewhat controversial, while both increase and decrease of connectivity have been detected [12,14-18,20]. The controversial findings in functional connectivity between different mutation carriers may be explained by neuroanatomical and neuropathological differences between the genetically driven disease groups, severity of the disease and small sample size in all genetic studies. Also the variability of rfMRI methods can have an impact on the results and makes it difficult to compare results.

BvFTD is a neuroanatomically heterogeneous group of syndromes compared with typical AD where the atrophy is more consistent. The location of brain atrophy and also clinical symptoms seem to be different between patients with the *C9ORF72*-, *MAPT*- or *PGRN*-mutations and in sporadic FTLD. The *C9ORF72* expansion is typically associated with symmetrical and widespread atrophy predominantly in frontal lobes, with additional involvement of the anterior temporal and parietal lobes and cerebellum [39], while patients with *MAPT* and *PGRN* mutations have shown more prominent temporal atrophy [40]. Interestingly, the type of atrophy is not unanimous between the patients with the *C9ORF72* expansion and there is substantial variability between subjects in the imaging findings of the *C9ORF72* associated FTLD, which may have an effect on fMRI findings at group level even in patients with the same genetic background [36,41,42]. In the present study gray matter atrophy was detected pre-dominantly in right frontal lobe, but also mildly in left temporo-parietal regions. Similar types of atrophy and metabolic changes have been detected in quantitative meta-analysis of voxel-based morphometry and positron emission tomography in patients with bvFTD [43].

The strength of the current study is the use of ICA that is able to separate noise sources from neurophysiological signals making the analysis more sensitive. Also the gray matter volumes were used as regressors to minimize the effects of atrophy on the functional connectivity analysis. The main limitation of this study is the small sample size of patients due to rare disease. In previous reports, the

number of genetically confirmed bvFTD patients has also been limited and comparable to our study [15,16,20]. However, even in a small cohort, we found functional changes in several relevant cognitive networks which can be thought to explain the symptoms of bvFTD.

This is the first report of fMRI-changes in bvFTD patients with the *C9ORF72* expansion. Our results of increased anti-correlation between the DMN and the thalamic regions of the salience network confirm previous findings of the role of these two networks also in bvFTD patients with a new genetic background. Increased functional connectivity was detected in the dorsal attention network and the salience network. These changes are suitable to explain neuropsychiatric symptoms and cognitive defects of patients with bvFTD. However, there is a lot of variation between findings in different studies and further investigations with larger patient groups are needed to clarify the balance of the main cognitive networks in this heterogeneous patient group.

Acknowledgement

Dr. Traynor has a patent pending on the diagnostic and therapeutic uses based on the discovery of the hexanucleotide repeat expansion in *C9ORF72*. The remaining authors disclose no conflicts of interest.

This work was supported by grants from Finnish Academy grants 117111 and 123772 (VK), Finnish Medical Foundation (VK, AMR), Finnish Neurological Foundation (VK), KEVO grants from Oulu University hospital (VK, AMR), National Graduate School of Clinical Investigation (RR), the Intramural Research Programs of the NIH and National Institute on Aging (Z01-AG000949-02) (BT) the ALS Association, AriSLA, Packard Center for ALS research, FIGC, Microsoft Research (BT) and the Myasthenia Gravis Foundation (BT).

References

1. Neary D, Snowden J, Mann D (2005) Frontotemporal dementia. Lancet Neurol 4: 771-780.
2. Rascovsky K, Hodges JR, Knopman D, Mendez MF, Kramer JH, et al. (2011) Sensitivity of revised diagnostic criteria for the behavioural variant of frontotemporal dementia. Brain 134: 2456-2477.
3. Cruts M, Theuns J, Van Broeckhoven C (2012) Locus-specific mutation databases for neurodegenerative brain diseases. Hum Mutat 33: 1340-1344.
4. DeJesus-Hernandez M1, Mackenzie IR, Boeve BF, Boxer AL, Baker M, et al. (2011) Expanded GGGGCC hexanucleotide repeat in noncoding region of C9ORF72 causes chromosome 9p-linked FTD and ALS. Neuron 72: 245-256.
5. Renton AE, Majounie E, Waite A, Simón-Sánchez J, Rollinson S, et al. (2011) A hexanucleotide repeat expansion in C9ORF72 is the cause of chromosome 9p21-linked ALS-FTD. Neuron 72: 257-268.
6. Pievani M, de Haan W, Wu T, Seeley WW, Frisoni GB (2011) Functional network disruption in the degenerative dementias. Lancet Neurol 10: 829-843.
7. Biswal B, Yetkin FZ, Haughton VM, Hyde JS (1995) Functional connectivity in the motor cortex of resting human brain using echo-planar MRI. Magn Reson Med 34: 537-541.
8. Fox MD, Raichle ME (2007) Spontaneous fluctuations in brain activity observed with functional magnetic resonance imaging. Nat Rev Neurosci 8: 700-711.
9. Seeley WW, Menon V, Schatzberg AF, Keller J, Glover GH, et al. (2007) Dissociable intrinsic connectivity networks for salience processing and executive control. J Neurosci 27: 2349-2356.
10. Seeley WW, Crawford RK, Zhou J, Miller BL, Greicius MD (2009) Neurodegenerative diseases target large-scale human brain networks. Neuron 62: 42-52.
11. Whitwell JL, Josephs KA (2012) Recent advances in the imaging of frontotemporal dementia. Curr Neurol Neurosci Rep 12: 715-723.
12. Zhou J, Greicius MD, Gennatas ED, Growdon ME, Jang JY, et al. (2010) Divergent network connectivity changes in behavioural variant frontotemporal dementia and Alzheimer's disease. Brain 133: 1352-1367.
13. Binnewijzend MA, Schoonheim MM, Sanz-Arigita E, Wink AM, van der Flier WM, et al. (2012) Resting-state fMRI changes in Alzheimer's disease and mild cognitive impairment. Neurobiol Aging 33: 2018-2028.
14. Filippi M, Agosta F, Scola E, Canu E, Magnani G, et al. (2013) Functional network connectivity in the behavioral variant of frontotemporal dementia. Cortex 49: 2389-2401.
15. Borroni B, Alberici A, Cercignani M, Premi E, Serra L, et al. (2012) Granulin mutation drives brain damage and reorganization from preclinical to symptomatic FTLD. Neurobiol Aging 33: 2506-2520.
16. Whitwell JL, Josephs KA, Avula R, Tosakulwong N, Weigand SD, et al. (2011) Altered functional connectivity in asymptomatic MAPT subjects: a comparison to bvFTD. Neurology 77: 866-874.
17. Rytty R, Nikkinen J, Paavola L, Abou Elseoud A, Moilanen V, et al. (2013) GroupICA dual regression analysis of resting state networks in a behavioral variant of frontotemporal dementia. Front Hum Neurosci 7: 461.
18. Farb NA, Grady CL, Strother S, Tang-Wai DF, Masellis M, et al. (2013) Abnormal network connectivity in frontotemporal dementia: evidence for prefrontal isolation. Cortex 49: 1856-1873.
19. Thompson PM, Martin NG, Wright MJ (2010) Imaging genomics. Curr Opin Neurol 23: 368-373.
20. Dopper EG, Rombouts SA, Jiskoot LC, Heijer Td, de Graaf JR, et al. (2013) Structural and functional brain connectivity in presymptomatic familial frontotemporal dementia. Neurology 80: 814-823.
21. Piguet O, Hornberger M, Mioshi E, Hodges JR (2011) Behavioural-variant frontotemporal dementia: diagnosis, clinical staging, and management. Lancet Neurol 10: 162-172.
22. Jenkinson M, Bannister P, Brady M, Smith S (2002) Improved optimization for the robust and accurate linear registration and motion correction of brain images. Neuroimage 17: 825-841.
23. Smith SM (2002) Fast robust automated brain extraction. Hum Brain Mapp 17: 143-155.
24. Beckmann CF, Smith SM (2004) Probabilistic independent component analysis for functional magnetic resonance imaging. IEEE Trans Med Imaging 23: 137-152.
25. Abou-Elseoud A, Starck T, Remes J, Nikkinen J, Tervonen O, et al. (2010) The effect of model order selection in group PICA. Hum Brain Mapp 31: 1207-1216.
26. Littow H, Elseoud AA, Haapea M, Isohanni M, Moilanen I, et al. (2010) Age-Related Differences in Functional Nodes of the Brain Cortex - A High Model Order Group ICA Study. Front Syst Neurosci 4.
27. Smith SM, Fox PT, Miller KL, Glahn DC, Fox PM, et al. (2009) Correspondence of the brain's functional architecture during activation and rest. Proc Natl Acad Sci U S A 106: 13040-13045.
28. Filippini N, MacIntosh BJ, Hough MG, Goodwin GM, Frisoni GB, et al. (2009) Distinct patterns of brain activity in young carriers of the APOE-epsilon4 allele. Proc Natl Acad Sci U S A 106: 7209-7214.
29. Nichols TE, Holmes AP (2002) Nonparametric permutation tests for functional neuroimaging: a primer with examples. Hum Brain Mapp 15: 1-25.
30. Allen EA, Damaraju E, Plis SM, Erhardt EB, Eichele T, et al. (2014) Tracking whole-brain connectivity dynamics in the resting state. Cereb Cortex 24: 663-676.
31. Abou Elseoud A, Nissilä J, Liettu A, Remes J, Jokelainen J, et al. (2014) Altered resting-state activity in seasonal affective disorder. Hum Brain Mapp 35: 161-172.
32. Fox MD, Snyder AZ, Vincent JL, Corbetta M, Van Essen DC, et al. (2004) The human brain is intrinsically organized into dynamic, anticorrelated functional networks. Proc NatlAcad Sci U S A 102(27):9673-9678
33. Seeley WW, Allman JM, Carlin DA, Crawford RK, Macedo MN, et al. (2007) Divergent social functioning in behavioral variant frontotemporal dementia and Alzheimer's disease: reciprocal networks and neuronal evolution. Alzheimer Dis Assoc Disord 21(4):S50-57
34. Schmahmann JD, Pandya DN (2008) Disconnection syndromes of basal ganglia, thalamus, and cerebrocerebellar systems. Cortex 44: 1037-1066.
35. Irwin DJ, McMillan CT, Brettschneider J, Libon DJ, Powers J, et al. (2013) Cognitive decline and reduced survival in C9ORF72 expansion frontotemporal degeneration and amyotrophic lateral sclerosis. J Neurol Neurosurg Psychiatry 84: 163-169.
36. Mahoney CJ, Beck J, Rohrer JD, Lashley T, Mok K, et al. (2012) Frontotemporal

dementia with the C9ORF72 hexanucleotide repeat expansion: clinical, neuroanatomical and neuropathological features. Brain 135: 736-750.

37. Fox MD, Corbetta M, Snyder AZ, Vincent JL, Raichle ME (2006) Spontaneous neuronal activity distinguishes human dorsal and ventral attention systems. Proc Natl Acad Sci U S A 103: 10046-10051.

38. Li R, Wu X, Fleisher AS, Reiman EM, Chen K, et al. (2012) Attention-related networks in Alzheimer's disease: a resting functional MRI study. Hum Brain Mapp 33: 1076-1088.

39. Whitwell JL, Weigand SD, Boeve BF, Senjem ML, Gunter JL, et al. (2012) Neuroimaging signatures of frontotemporal dementia genetics: C9ORF72, tau, progranulin and sporadics. Brain 135: 794-806.

40. Whitwell JL, Przybelski SA, Weigand SD, Ivnik RJ, Vemuri P, et al. (2009) Distinct anatomical subtypes of the behavioural variant of frontotemporal dementia: a cluster analysis study. Brain 132: 2932-2946.

41. Boeve BF, Boylan KB, Graff-Radford NR, DeJesus-Hernandez M, Knopman DS, et al. (2012) Characterization of frontotemporal dementia and/or amyotrophic lateral sclerosis associated with the GGGGCC repeat expansion in C9ORF72. Brain 135: 765-783.

42. Kaivorinne AL, Bode MK, Paavola L, Tuominen H, Kallio M, et al. (2013) Clinical Characteristics of C9ORF72-Linked Frontotemporal Lobar Degeneration. Dement Geriatr Cogn Dis Extra 3: 251-262.

43. Zhou J, Seeley WW2 (2014) Network dysfunction in Alzheimer's disease and frontotemporal dementia: implications for psychiatry. Biol Psychiatry 75: 565-573.